

Electronic Supplementary Information (ESI) for

Complex oscillatory decrease with size in diffusivity of {100}-epitaxially supported 3D fcc metal nanoclusters

King C. Lai and James W. Evans

Division of Chemical & Biological Sciences, Ames Laboratory, USDOE and
Department of Physics & Astronomy, Iowa State University, Ames IA 50011

Nanoscale (The Royal Society of Chemistry)

1. Parameters for stochastic lattice-gas model for various fcc metals

While all results in this paper were presented with model parameters corresponding to Ag NCs, the model applies generally for fcc metals. Appropriate kinetic parameters, C_{TD100} , C_{TD111} , C_{ED111B} , and $C_{ED111A} = C_{ED100}$, for Au, Pt, and Pd (as well as Ag), are shown in **Table 1**. In addition, suitable values must be assigned for the effective NN interaction, ϕ , and for the additional Ehrlich-Schwoebel barrier for downward interlayer diffusion, δ_{ES} , for step edges where this barrier is non-zero. Reasonable values are: $\phi = 0.225$ eV and $\delta_{ES} = 0.10$ eV and for Ag; $\phi = 0.22$ eV and $\delta_{ES} = 0.12$ for Au; and $\phi = 0.43$ eV and $\delta_{ES} = 0.35$ for Pt. For Pd, one could set $\phi = 0.22$ eV, but a reliable value for δ_{ES} is not currently available. See K.C. Lai, Y. Han, P. Spurgeon, W. Huang, P.A. Thiel, D.-J. Liu and J.W. Evans, Reshaping, Intermixing, and Coarsening for Metallic Nanocrystals: Non-equilibrium Statistical Mechanical and Coarse-grained Modeling, *Chemical Reviews* 2019, **119**, 6670-6768.

Table 1. Parameters for the stochastic lattice-gas model for various fcc metals.

	C_{TD100}	C_{TD111}	C_{ED111B}	$C_{ED111A} = C_{ED100}$
Ag	0.425	0.10	0.30	0.275
Au	0.40	0.125	0.375	0.45
Pt	0.47	0.26	0.84	0.90
Pd	0.75	0.35	0.39	0.48

2. Neglect of detachment in the stochastic lattice-gas model

Our choice of model dynamics allows diffusion of metal atoms across the nanocluster (NC) surface, but not detachment of atoms from the NC at its base, diffusion across the substrate, and possible reattachment to the NC. Here, we provide multiple perspectives on why the detachment process can reasonably be ignored.

(i) For diffusion across the NC surface, one regards extraction from a kink to the terrace as the rate controlling processes with an effective barrier of E_d (terrace diffusion barrier) + ΔE (energy change). This yields 0.775 eV [0.875 eV] for (111) [(100)] terraces in our model. For detachment from (a kink site on) the nanocluster to the substrate, the effective barrier is E_d (substrate) + $\{\Delta E = (6-4f)\phi\}$. This yields 1.10 eV [1.32 eV] in our

modeling with strong $f = 0.75$ [weak $f \approx 0.05$] adhesion. These barriers are sufficiently high relative to surface diffusion to justify neglect of detachment.

(ii) In related studies of the reshaping of metal nanoparticles, it has long been argued that surface diffusion (rather than various other possible mechanisms) is the dominant pathway for mass transport in the sub-micron size regime. This view goes back to classic studies by Herring, Mullins & Nicholis, et al., as noted more recently by Eggers [J. Eggers, Coalescence of Spheres by Surface Diffusion, *Phys. Rev. Lett.* 1980, **80**, 2634-2637].

(iii) In the case of strong adhesion corresponding to metal(100) homoepitaxy ($f = 1$) associated with 2D (100)-epitaxially supported NCs, there are extensive experimental studies, and also extensive ab-initio level modeling, demonstrating that periphery diffusion (the 1D analogue of surface diffusion) and not attachment-detachment dominate mass transport, and in particular NC diffusion. See the review P.A. Thiel, M. Shen, D.-J. Liu and J.W. Evans, Coarsening of two-dimensional nanoclusters on metal surfaces, *J. Phys. Chem C* 2009, **113**, 5047-5067.

3. KMC simulation results for time-dependent NC diffusivity: $f = 0.75$

Figure S1 shows KMC simulation results for the time dependent NC diffusion coefficient, as $D_N(\delta t) = \langle \delta r_{CM}(\delta t) \cdot \delta r_{CM}(\delta t) \rangle / (4\delta t)$ for the case of strong adhesion, $f = 0.75$, at 900 K. Specifically, results for $D_N(\delta t)$ versus δt are shown for the NC size range $N = 93 - 97$. As discussed in the text, $D_N(\delta t)$ decreases monotonically from an initially high value for short δt to a plateau value corresponding to the true NC diffusion coefficient, D_N , for δt exceeding $\delta t_p \approx 1-2 \times 10^6/v$. To obtain reliable values for $D_N(\delta t)$ with $\delta t \approx \delta t_p$, simulations are run to obtain CM trajectories for a total length of time of 200 δt_p .

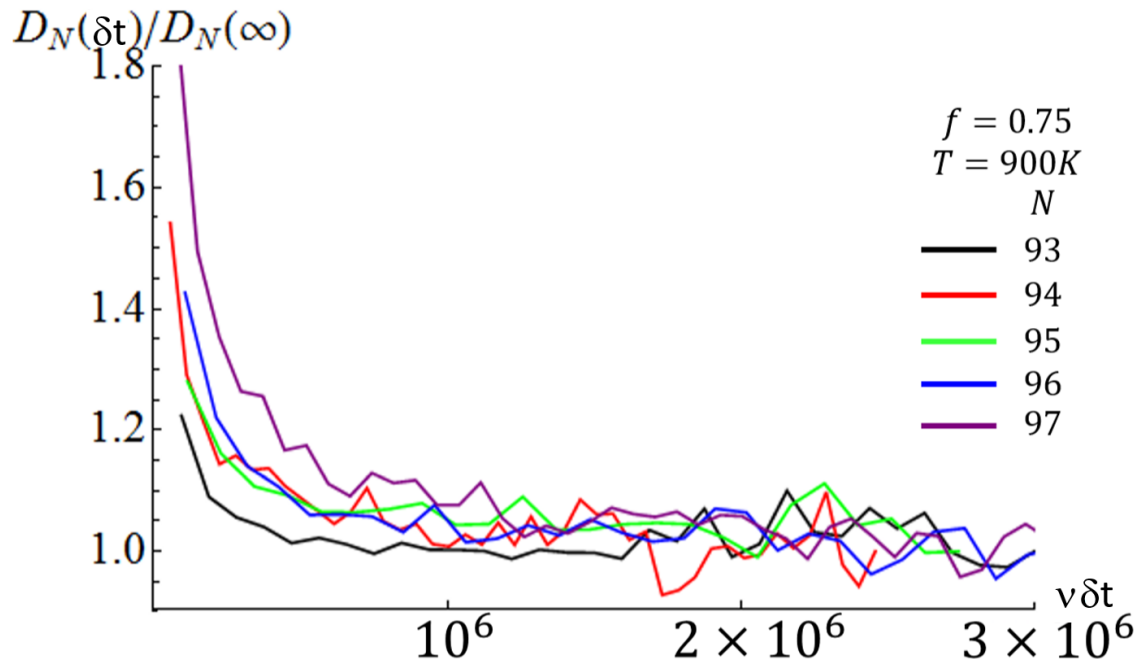


Figure S1. KMC simulation results for the time-dependent NC diffusion coefficient, $D_N(\delta t)$, versus δt for $f = 0.75$ at 900 K for sizes, N , as indicated.

4. NC configurations during diffusion from KMC simulation

In **Figure S2**, we present snapshots from KMC simulation showing a sequence of NC configurations during diffusion for the case of $N = 50$ with strong adhesion, $f = 0.75$, at 900 K.

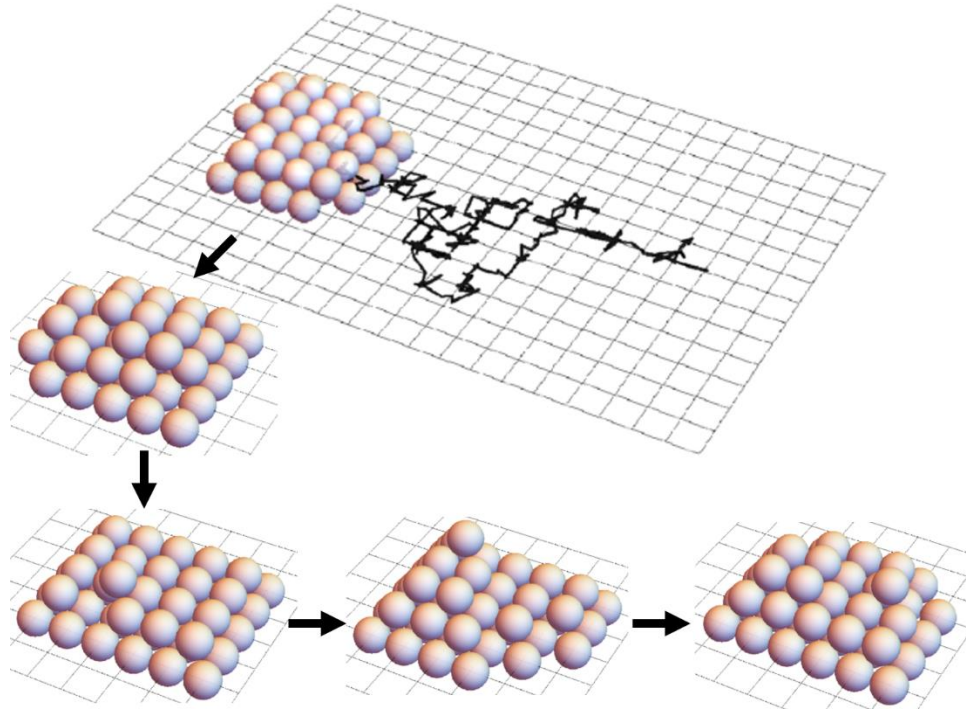


Figure S2. Snapshots from KMC simulation showing a sequence of NC configurations during diffusion for the case $N = 50$ with strong adhesion, $f = 0.75$, at 900 K.

5. KMC simulation results for D_N for $f = 0.75$ at 900 K for larger sizes

Results shown in **Figure S3** (bottom frame) demonstrate that the basic features shown in Figure 3 for D_N versus N with $f = 0.75$ up to $N \approx 190$, i.e., complex oscillatory decay of D_N versus N , are preserved for larger N . Note that the additional results for D_N only correspond to a subset of closed-shell TPs (TP_{8x8,4}, TP_{8x8,5}, TP_{8x9,4}, TP_{8x9,5}, TP_{9x9,5}, TP_{9x10,5}, TP_{10x10,5}, TP_{10x10,6}, TP_{10x11,6}, TP_{11x11,6}, TP_{11x12,6}, TP_{12x12,6}, TP_{12x12,7}, TP_{12x13,6}, TP_{12x13,7}, TP_{13x13,7}, and TP_{13x14,7}). Local minima in D_N only occur for subset of these. An effective criterion to assess this subset of closed-shell sizes corresponding to local minima in D_N is again provided by (the occurrence of local minima in) the readily calculated quantity, $\delta E = \delta E_N$, the deviation from the continuum form of the energy per atom. δE versus N is also shown in **Figure S3** (top).

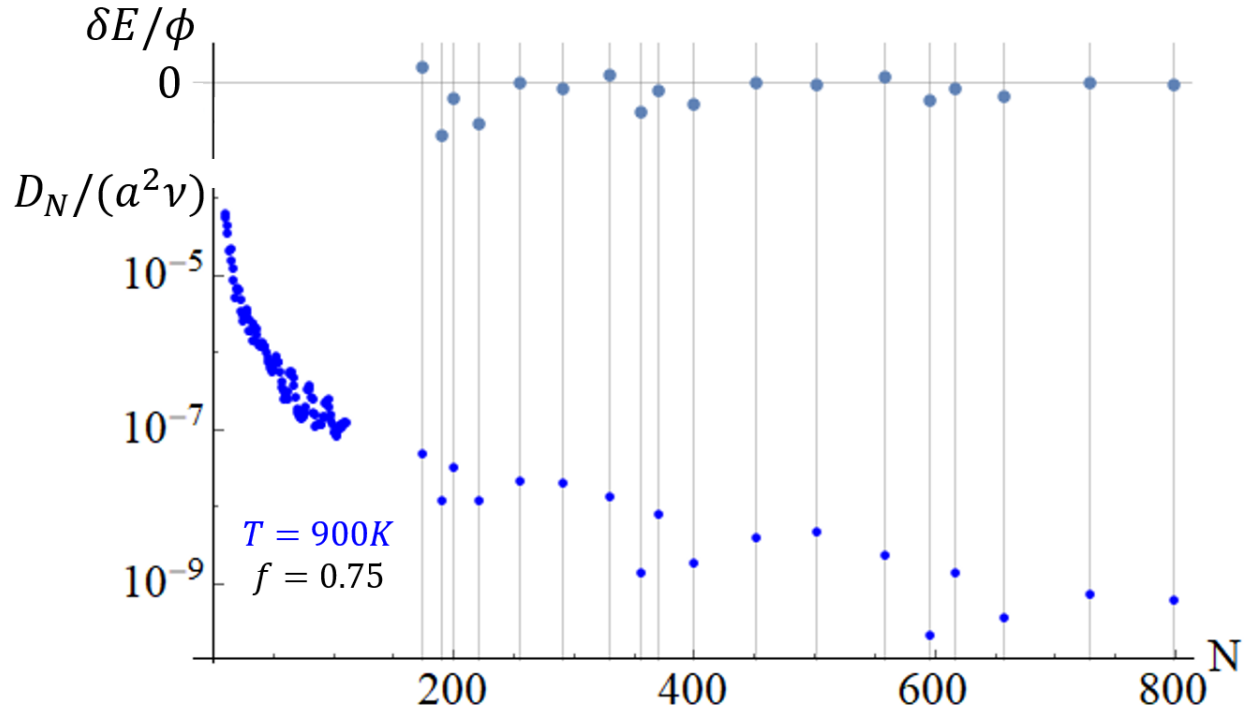


Figure S3. Top: $\delta E = [E_N - E_N(\text{cont})]/N$ where $E_N(\text{cont})/\phi = 0.529 - 1.496N^{1/3} + 3.977N^{2/3} - 6N$ recovers E_N for TP_{3x3,3}, TP_{5x5,3}, TP_{7x7,4}, and TP_{9x9,5}. Middle: KMC results for D_N versus N for an Ag NCs with $f = 0.75$ at 900 K.

6. Diffusion pathways via NC heights differing from the ground state

Figure S4 shows results for $\Delta E(\text{max})$ versus NC size N for strong adhesion ($f = 0.75$) now discriminating between mass transfer pathways involving different NC heights (i.e., heights which may differ from that of the ground state NC configuration). This analysis shows that the diffusion pathway constrained to NCs with the same height as the ground state (GS) configuration may not always be the one with lowest energy barrier. Examples are provided by: the 2-layer diffusion path for $N = 36$ (3-layer GS); the 3-layer diffusion path for $N = 54$ (4-layer GS); the 3-layer diffusion path for $N = 66$ (4-layer GS). Below, we discuss the latter case in more detail.

Figure S5 provides a more detailed illustration of energetics, specifically $\Delta E(q)$ versus the number, q , of transferred atoms, for $N = 66$ (4-layer GS) where a diffusion pathway through 3-layer structures yields a lower barrier than one constrained to 4-layers. For this 3-layer pathway, shown in blue, the first for $q = 1-4$ corresponds to the transformation of the 4-layer ground state structure (TP_{5x6,4} with 2 atoms removed) to a 3-layer configuration (TP_{5x6,4} with 4 atoms added), then subsequent $q = 5, 6, \dots$ correspond to transferring atoms from one side to another in 3-layer structures, and $q = 17-20$ correspond to recovering the 4-layer ground state structure from a 3-layer structure. Energetics mid-way between transfer of each atom is not included in this plot.

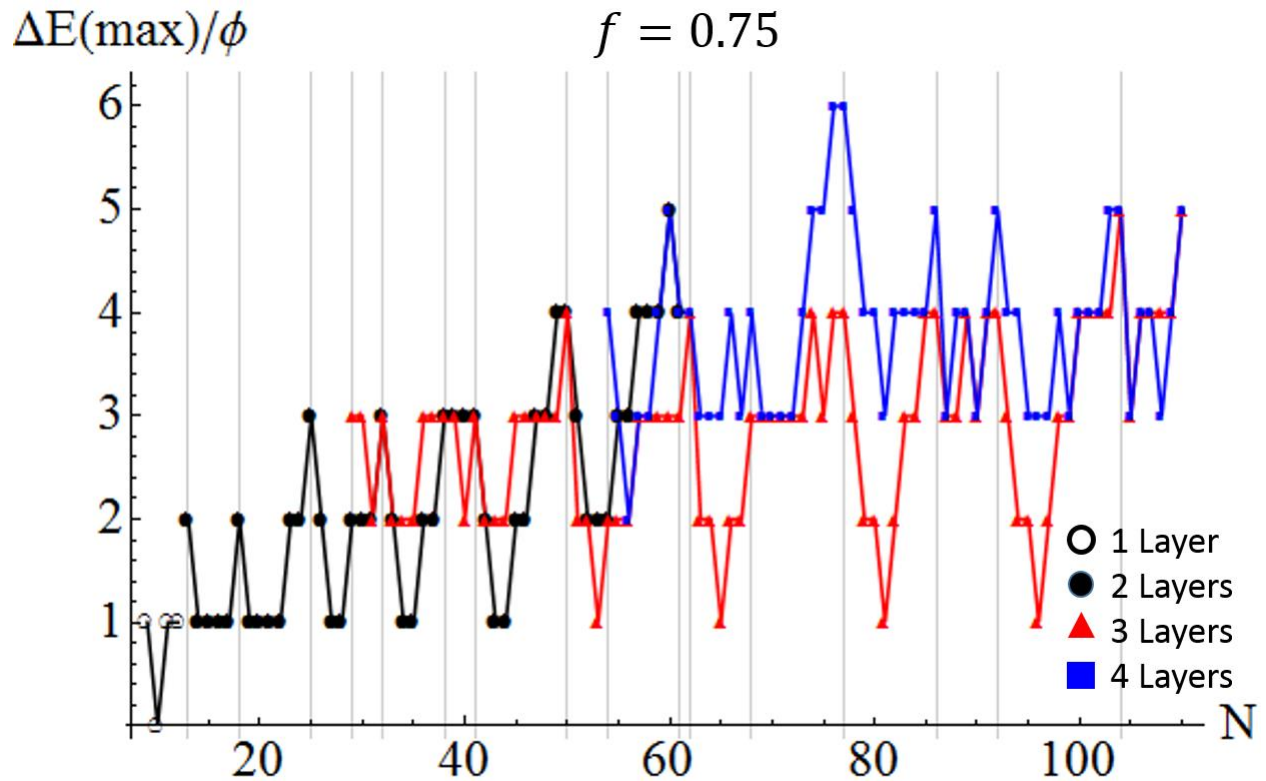


Figure S4. Analytic results for $\Delta E(\max)$ for $f = 0.75$ for NC diffusion through configuration spaces with various constrained numbers of layers.

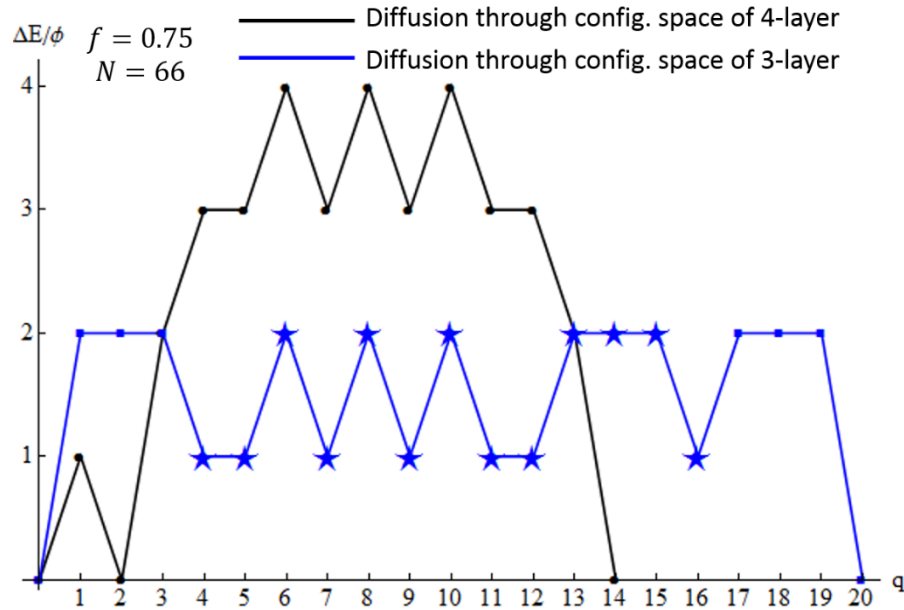


Figure S5. $\Delta E(q)$ for diffusion of an $N = 66$ NC through a configuration space constrained to four layers (black) or allowed to access three layer structures (blue). Stars indicate NCs in a 3-layer configuration.

7. Continuum analysis of energetics during atom transfer: $f = 0.75$

For the simplest case of a closed-shell (CS) truncated pyramid (TP), as atoms are transferred from one initially complete layer on a {111} side facet to another side, partially complete layers or 2D islands are formed on outer edges. Thus, in tracking the energy along the MEP during mass transfer, a basic issue is the equilibrium structure or shape of these 2D islands. It is clear that one side of the island will correspond to the contact line base of the TP, so that the atoms along that edge can exploit bonding to substrate atoms. The other edges naturally have standard close-packed structure for islands on {111} facets. Thus, the island structure is as shown in **Figure S6**. However, it is still necessary to assess the explicit equilibrium shape as determined by the ratio of the side to top edge lengths, s/t . This ratio is determined by the ratio of the step energy of the side and top edges relative to the effective step energy of the bottom edge.

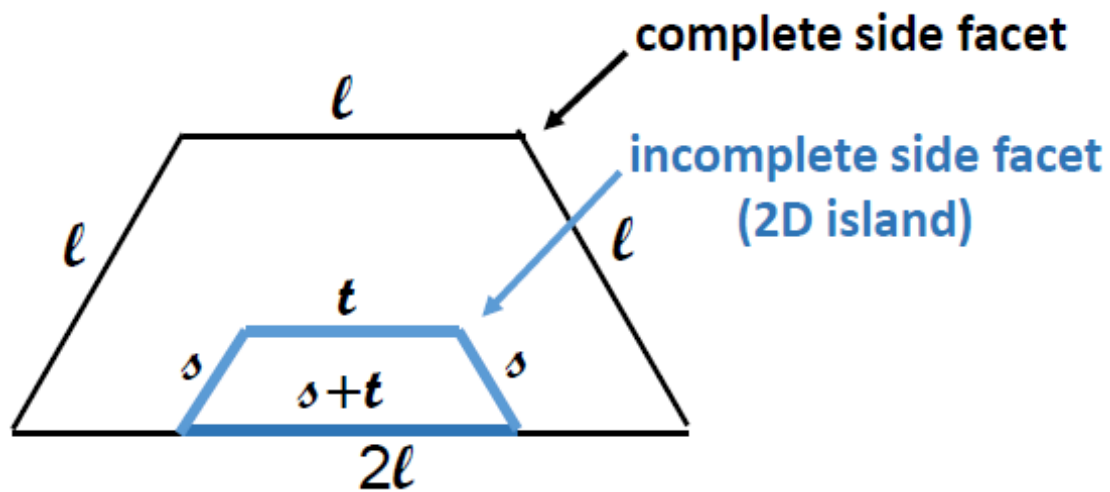


Figure S6. Analysis of equilibrium shape of a 2D island on a {111} side facet.

For atoms in the interior of the 2D island, we assign an energy of

$$E_c = E_c(\text{lateral NC}) + E_c(\text{support NC}) = -6\phi,$$

where $E_c(\text{lateral NC}) = -6\phi/2$ (6 shared bonds with lateral NC neighbors, where here “lateral” means in the plane of the 2D island), and $E_c(\text{support NC}) = -3\phi$ (3 non-shared bonds to NC atoms in the “supporting” {111} side facet). For atoms at the side or top edges, we assign an energy

$$E_{s,t} = E_{s,t}(\text{lateral NC}) + E_{s,t}(\text{support NC}) = -5\phi,$$

where $E_{s,t}(\text{lateral NC}) = -4\phi/2$ (corresponding to 4 shared bonds with lateral NC neighbors, since now 2 lateral NC neighbors are missing) and $E_{s,t}(\text{support NC}) = -3\phi$ (3 non-shared bonds to NC atoms in the “supporting” {111} side facet, as above).

Consequently, the side and top step energies are given by $\sigma_{s,t} = E_{s,t} - E_c = \phi$ per atom. For atoms at the bottom edge, we assign an energy

$$E_b = E_b(\text{lateral NC}) + E_b(\text{lateral sub}) + E_b(\text{support NC}) + E_b(\text{support sub}) = -6\phi.$$

Here, $E_{s,t}(\text{lateral NC}) = -4\phi/2$ (corresponding to 4 shared bonds with lateral NC neighbors), $E_{s,t}(\text{lateral sub}) = -2 \times (0.75\phi)$ (2 non-shared bonds of strength 0.75ϕ to lateral substrate atoms), $E_b(\text{support NC}) = -\phi$ (1 non-shared bond to a supporting NC atom), and $E_b(\text{support sub}) = -2 \times (0.75\phi)$ (2 non-shared bond of strength 0.75ϕ to a supporting substrate atom). Thus, the effective step energy per atom for the bottom step is $\sigma_b = E_b - E_c = 0$. Essentially the higher coordination of atoms at the bottom step overcompensates for the weaker bonding to substrate atoms to result in this vanishing effective step energy.

Now given the equal non-zero step energy for the side and top steps, and the vanishing effective step energy for the bottom step, minimization of the total energy for the 2D island of fixed area immediately reveals that side and top steps have the same length, i.e., that $s = t$. Thus, the final intuitively natural result is that the shape of the 2D island is the same as the shape of the overall side facets of the TP.

8. Continuum analysis for open-shell NCs: $f = 0.75$

Our continuum treatment for open-shell (OS) TPs analyzes variation in NC energetics for a NC diffusion mechanism involving mass transfer in two stages. In the first, atoms are transferred from a complete facet 1 to grow an initially incomplete layer on facet 2 (which becomes complete). In the second, the incomplete layer remaining on facet 1 is transferred to facet 2. Below, x_1 (x_2) denotes the fraction of atoms transferred in the first (second) stage. Then the energy variation in stage 1 is given by

$$\Delta E(x_1)|_{\text{os}} = [\{r^2 + (1-r^2)x_1\}^{1/2} - r - 1 + \{1 - (1-r^2)x_1\}]3\sigma\ell$$

leading to $\Delta E(\text{max1})|_{\text{os}} = [\sqrt{2}(1+r^2)^{1/2} - r - 1]3\sigma\ell$ for $x_1 = \frac{1}{2}$. Then, the energy variation in stage 2 is given by

$$\Delta E(x_2)|_{\text{os}} = 3r\sigma\ell [(1-x_2)^{1/2} + (x_2)^{1/2} - 1] \text{ leading to } \Delta E(\text{max2})|_{\text{os}} = 3(\sqrt{2} - 1)r\sigma\ell \text{ for } x_2 = \frac{1}{2}.$$

9. Degeneracy of initial & transition states for NC diffusion: $f = 0.75$

Here, we consider diffusion of a TP for $f = 0.75$. Based on the general heuristic formula, $D_N \sim (\Omega_{\text{TS}}/\Omega_0) \exp[-E_{\text{eff}}(\text{analytic})/(k_B T)]$, from Kramer's reaction rate theory, it is clear that the actual value of the diffusion coefficient will be impacted by the degeneracy Ω_0 of the ground state NC configuration, and the degeneracy, Ω_{TS} , of the transition state at $q \approx q_{\text{tot}}/2$ where half a complete layer has been transferred from one side of the NC to another. Of particular interest is comparison of D_N for closed shell TP with $N = N_{\text{TP}}$, and for TP with one or three less atoms, in cases where $E_{\text{eff}}(\text{analytic})$ is the same. Then entropic effects could lead to lower D_N for the non-closed shell structure. As noted in the text, $\Omega_0 = 1$ for $N = N_{\text{TP}}$ with a square base versus $\Omega_0 = 8$ for $N = N_{\text{TP}} - 1$. In the latter

case, the atom can be removed from one of the four top corners (breaking 6 bonds of strength ϕ with NC atoms) or from the four bottom corners (breaking 3 bonds of strength ϕ with NC atoms, and 4 bonds of strength 0.75ϕ with substrate atoms).

For the transition state, the determination of degeneracy is more complicated. However, as an example, we find that $\Omega_{TS} = 288$ for $N_{TP} = 126$ versus $\Omega_{TS} = 864$ for $N_{TP} - 1 = 125$. Thus, $\Omega_{TS}/\Omega_0 = 288$ for $N = N_{TP} = 126$ versus $\Omega_{TS}/\Omega_0 = 108$ for $N = N_{TP} - 1 = 125$ resulting in the lower D_N for the non-closed shell case.

10. Dissolution & build up of facets on supported TOs: weak adhesion

For analytic characterization of the NC energetics along the MEP for diffusion of a weakly supported TO, various possibilities must be considered for dissolution of two $\{100\}$ and $\{111\}$ facets by transfer of atoms to two other $\{100\}$ and $\{111\}$ facets. Below, we present the relevant analysis for a regular closed-shell TO with magic size $N = N_{TO} = 201$, where one removes atoms from a $\{111\}$ then a $\{100\}$ then a $\{100\}$ and finally a $\{111\}$ facet, and builds up layers in the reverse sequence (first on a $\{100\}$ etc.) to obtain $\Delta E(\max) = 6\phi$. **Figure S7** shows the number of broken bonds for each removed atom as a total of $q = 1 - 43$ atoms are sequentially removed from the four facets in the order described above. Accounting for the feature that atoms are added to the four other facets in the reverse order of removal, from **Figure S7** one can construct $\Delta E(q)$ versus q . Results are shown in **Figure S8** demonstrating that $\Delta E(\max) = 6\phi$, as stated above.

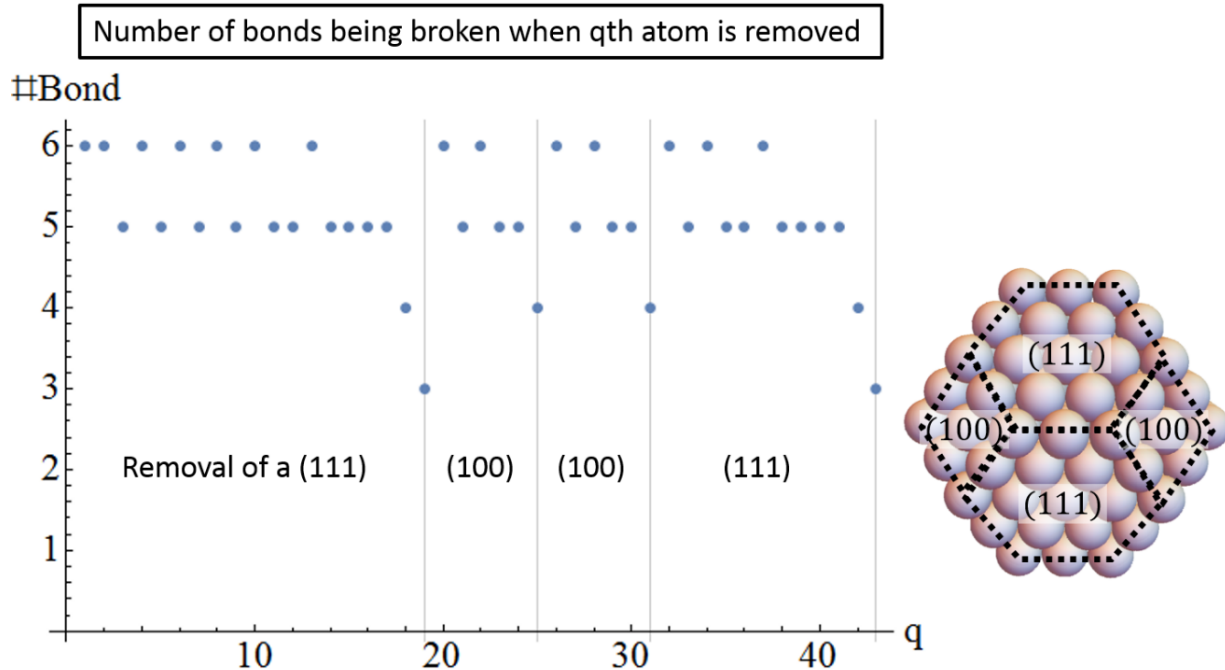


Figure S7. Analysis of the number of broken bonds upon removal of the q^{th} atom from outer facets on one side of a TO with $N = 201$, where these atoms reform layers on the other side during diffusion of the TO.

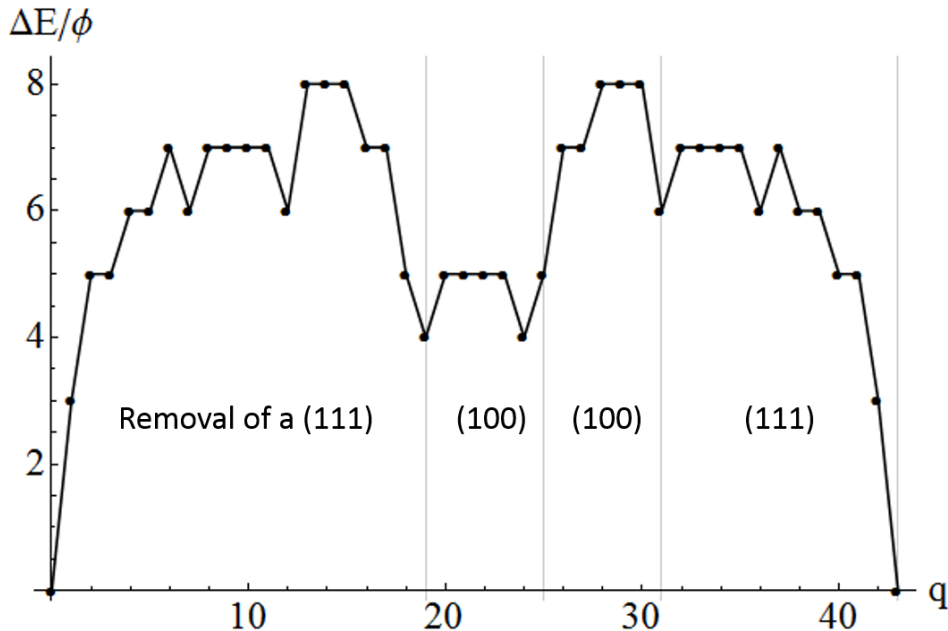


Figure S8. Analysis of the net number of broken bonds during the atom transfer process characterized in Figure S7 which leads to diffusion of TOs with $N = 201$.

11. Examples of particularly stable slow-diffusing NCs: $f \leq 0.05$

Our analysis of NC diffusion for weak adhesion $f \leq 0.05$ reveals that D_N displays prominent minima not just for regular TO structures and TO+ structures, but also for what we have described as “elongated” TO and for slab-like structures with 3-fold symmetry. **Figure S9** provides examples of these four structures.

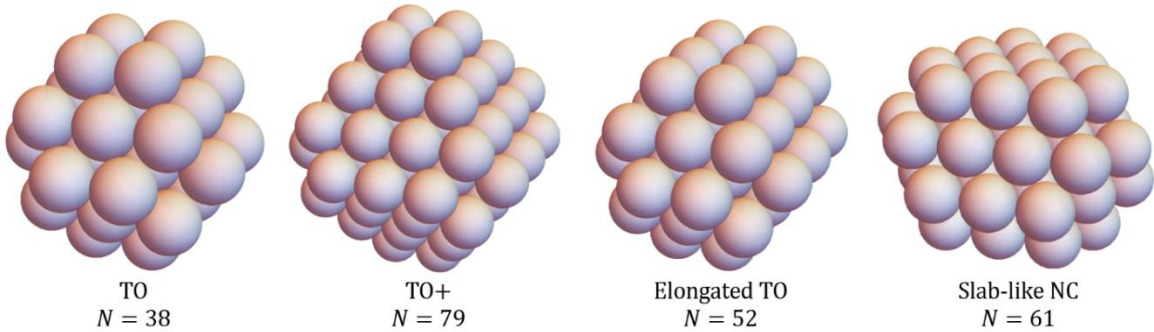


Figure S9: Examples of regular TO, TO+, elongated TO, and slab-like NC structures

12. NC diffusion and energetics for moderate adhesion $f = 0.5$

We have performed a detailed KMC simulation analysis of D_N versus N for NC diffusion with moderate adhesion $f = 0.5$. Results are shown in **Figure S10** (top). In addition, we have performed an analytic characterization of energetics along the MEP leading to the results for E_{eff} also shown in **Figure S10** (bottom). There is a good correlation between maxima (minima) in E_{eff} and minima (maxima) in D_N .

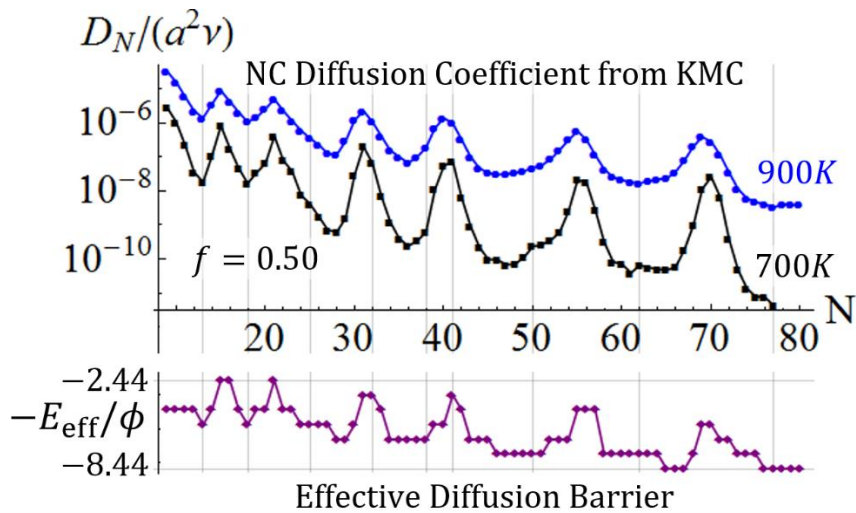


Figure S10. KMC simulation results for D_N versus N for NC diffusion with moderate adhesion $f = 0.50$ (top). Analytic determination of E_{eff} (bottom).

13. Ag NC diffusion on MgO(001) with $f = 0.17$ (compared with $f \approx 0$)

Experimental analysis indicates that Ag adhesion on MgO(001) is characterized by $f = 0.17$. Thus, we have performed KMC simulation of this case where C_α for atoms in the lowest layer of the NC are determined by a linear interpolation between our choice for strong adhesion and for weak adhesion. Results at 900 K are shown in **Figure S11** (top). The features appearing in D_N versus N for Ag/MgO(001) with $f = 0.17$ can be correlated with those appearing for $f = 0$ also shown in **Figure S11** (bottom).

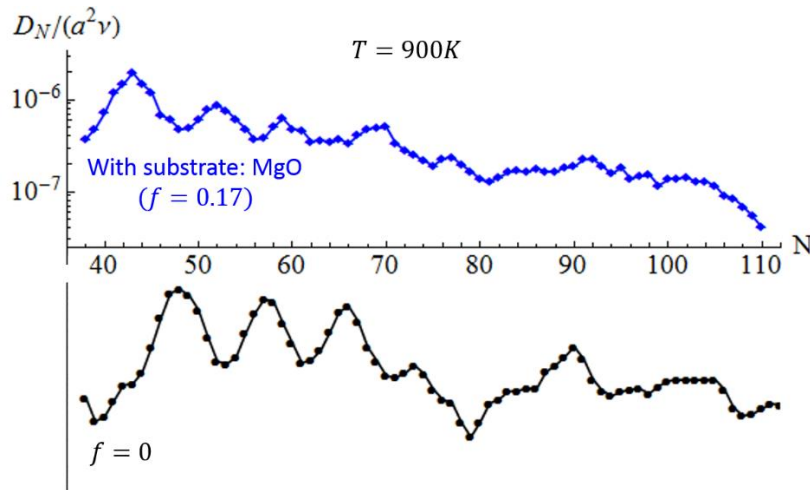


Figure S11. KMC simulation results for D_N versus N for diffusion of Ag NC on MgO(001) with $f = 0.17$ (top) at 900 K. Also shown are results for $f = 0$ at 900 K for comparison (bottom).

14. Tabulated values for D_N versus N

Table 2: KMC results of diffusion coefficient D_N with strong adhesion $f = 0.75$ at $T = 700K, 800K, and 900K.$

N	$f = 0.75$													
	700K			800K			900K	N	700K			800K		
	$D_N/(a^2\nu)$			$D_N/(a^2\nu)$			$D_N/(a^2\nu)$		$D_N/(a^2\nu)$			$D_N/(a^2\nu)$		
9	6.4487E-06	2.0541E-05	6.2279E-05	68	4.5343E-09	4.2087E-08	1.6295E-07							
10	6.2797E-06	2.1579E-05	5.4773E-05	69	2.2456E-09	2.8988E-08	1.9576E-07							
11	4.5186E-06	1.6930E-05	4.5090E-05	70	1.7414E-09	2.5242E-08	3.3847E-07							
12	3.0589E-06	1.3456E-05	3.6123E-05	71	1.0986E-09	1.9931E-08	3.8485E-07							
13	6.4820E-07	5.5510E-06	2.0648E-05	72	1.1805E-09	1.8776E-08	3.4534E-07							
14	1.0341E-06	6.3793E-06	2.2017E-05	73	8.2386E-10	1.6315E-08	2.6633E-07							
15	8.9632E-07	4.7895E-06	1.5522E-05	74	7.3443E-10	1.4743E-08	2.5305E-07							
16	7.1631E-07	3.5273E-06	1.2534E-05	75	9.9438E-10	1.8868E-08	1.6277E-07							
17	4.4125E-07	2.5591E-06	8.6826E-06	76	7.6738E-10	1.9849E-08	1.5979E-07							
18	1.1976E-07	1.1630E-06	5.0460E-06	77	9.7880E-10	2.3939E-08	1.1181E-07							
19	3.0827E-07	1.7109E-06	6.7107E-06	78	5.6564E-09	5.2752E-08	1.2021E-07							
20	3.9134E-07	2.1317E-06	6.8141E-06	79	1.5839E-08	1.0138E-07	1.1869E-07							
21	3.5881E-07	1.8793E-06	6.4495E-06	80	1.9598E-08	1.0380E-07	1.1663E-07							
22	2.1943E-07	1.2567E-06	4.9668E-06	81	1.3210E-08	6.6090E-08	1.2110E-07							
23	7.9815E-08	6.3803E-07	3.4538E-06	82	4.9875E-09	4.2489E-08	1.1835E-07							
24	6.1193E-08	5.9502E-07	3.0963E-06	83	2.5738E-09	2.5492E-08	1.4880E-07							
25	3.1307E-08	4.3455E-07	2.6353E-06	84	1.5911E-09	2.0250E-08	1.4966E-07							
26	1.3655E-07	8.1930E-07	3.2126E-06	85	9.7571E-10	1.6108E-08	2.2702E-07							
27	1.7411E-07	9.6185E-07	3.6555E-06	86	7.3105E-10	1.2729E-08	2.4361E-07							
28	1.6773E-07	7.9765E-07	3.2862E-06	87	8.3252E-10	1.4364E-08	2.5789E-07							
29	9.2457E-08	6.1613E-07	2.6937E-06	88	5.9111E-10	1.0373E-08	2.0531E-07							
30	4.1423E-08	4.0376E-07	1.9308E-06	89	5.4376E-10	1.3774E-08	1.5796E-07							
31	2.9072E-08	3.7074E-07	1.8751E-06	90	5.9194E-10	1.2322E-08	1.3544E-07							
32	2.1902E-08	2.3857E-07	1.4064E-06	91	5.8699E-10	1.2253E-08	1.1607E-07							
33	6.7905E-08	4.5992E-07	2.3791E-06	92	5.2561E-10	1.4210E-08	9.4883E-08							
34	1.2081E-07	6.5322E-07	2.1767E-06	93	3.7904E-09	3.7408E-08	9.2726E-08							
35	1.1630E-07	6.2151E-07	2.0544E-06	94	8.6285E-09	6.5008E-08	8.5451E-08							
36	5.4430E-08	3.7279E-07	1.6895E-06	95	1.3008E-08	6.4829E-08	8.8179E-08							
37	2.9289E-08	2.7043E-07	1.4003E-06	96	8.7217E-09	5.3598E-08	1.0810E-07							
38	2.1042E-08	2.3063E-07	1.3187E-06	97	3.8619E-09	3.1558E-08	1.0250E-07							
39	2.1242E-08	2.0663E-07	1.2369E-06	98	2.0675E-09	2.1990E-08	1.1804E-07							
40	2.9516E-08	2.9180E-07	1.3382E-06	99	1.1343E-09	1.5096E-08	1.0852E-07							
41	2.1232E-08	2.2155E-07	1.2468E-06	100	7.0688E-10	1.2608E-08	1.2557E-07							
42	5.1308E-08	3.2523E-07	1.2265E-06	101	5.1170E-10	9.3466E-09	1.2560E-07							
43	4.7534E-08	3.2611E-07	1.2460E-06	102	5.2624E-10	7.8513E-09	1.2421E-07							
44	4.1499E-08	2.6631E-07	1.0346E-06	103	3.5762E-10	8.5521E-09	1.6295E-07							
45	2.3249E-08	1.7986E-07	8.4356E-07	104	4.0410E-10	8.8181E-09	1.9576E-07							

46	1.3114E-08	1.5150E-07	7.8180E-07	105	7.2363E-10	1.1395E-08	3.3847E-07
47	8.0377E-09	1.0275E-07	6.2040E-07	106	7.6814E-10	1.1085E-08	3.8485E-07
48	7.5165E-09	1.0638E-07	6.5525E-07	107	6.0205E-10	1.0921E-08	3.4534E-07
49	4.7180E-09	8.5128E-08	5.8106E-07	108	7.2416E-10	1.3396E-08	2.6633E-07
50	2.9128E-09	6.5622E-08	5.9002E-07	109	6.0502E-10	1.6031E-08	2.5305E-07
51	2.1611E-08	1.4981E-07	7.6125E-07	110	7.3278E-10	1.5126E-08	1.6277E-07
52	4.3535E-08	2.2811E-07	9.1672E-07	111	2.8516E-09		
53	4.8754E-08	2.4688E-07	7.7878E-07	112	5.2835E-09		
54	2.9309E-08	1.5891E-07	7.4879E-07	113	4.8847E-09		
55	1.2755E-08	9.7509E-08	5.5693E-07	114	3.0283E-09		
56	6.2084E-09	6.0976E-08	4.2369E-07	115	1.0396E-09		
57	3.4412E-09	5.0579E-08	3.5125E-07	116	5.2641E-10		
58	2.6770E-09	4.1952E-08	3.1543E-07	117	3.3461E-10		
59	2.0836E-09	3.5598E-08	2.4975E-07	118	2.8779E-10		
60	1.8538E-09	3.5623E-08	2.8670E-07	119	1.7874E-10		
61	1.3738E-09	2.7720E-08	2.5220E-07	120	1.7916E-10		
62	1.3287E-09	2.6545E-08	3.1346E-07	121	1.4898E-10		
63	1.0946E-08	9.8064E-08	5.4712E-07	122	1.1598E-10		
64	3.0924E-08	1.7356E-07	5.7076E-07	123	1.3371E-10		
65	4.1117E-08	1.7167E-07	5.6612E-07	124	1.5483E-10		
66	1.9408E-08	1.1559E-07	4.7336E-07	125	1.2817E-10		
67	8.8671E-09	7.2085E-08	3.6809E-07	126	2.2007E-10		

Table 3. Deviation of energy per atom from continuum value with strong adhesion $f = 0.75$.

N	$\delta E(\phi)$						
9	4.1704E-02	39	2.0588E-02	69	2.4547E-02	99	2.2920E-02
10	1.2343E-01	40	2.6682E-02	70	2.9689E-02	100	1.7200E-02
11	1.0247E-01	41	8.2281E-03	71	2.0641E-02	101	1.1611E-02
12	8.7509E-02	42	3.8405E-02	72	2.5771E-02	102	1.5952E-02
13	-8.1986E-15	43	4.4048E-02	73	1.7099E-02	103	1.0517E-02
14	6.9587E-02	44	4.9553E-02	74	8.6970E-03	104	5.2020E-03
15	6.4704E-02	45	3.2705E-02	75	1.3887E-02	105	1.9052E-02
16	6.1698E-02	46	3.8436E-02	76	5.8154E-03	106	1.3788E-02
17	6.0144E-02	47	2.2748E-02	77	-2.0138E-03	107	8.6380E-03
18	4.1670E-03	48	2.8644E-02	78	1.6030E-02	108	1.2857E-02
19	6.0191E-02	49	1.3985E-02	79	2.0990E-02	109	7.8393E-03
20	6.1361E-02	50	2.2737E-15	80	2.5856E-02	110	2.9268E-03
21	6.3088E-02	51	2.5864E-02	81	3.0630E-02	111	1.6135E-02
22	6.5258E-02	52	3.1583E-02	82	2.3121E-02	112	2.0192E-02
23	2.4300E-02	53	3.7163E-02	83	1.5820E-02	113	2.4191E-02
24	2.8911E-02	54	2.4093E-02	84	2.0624E-02	114	2.8132E-02
25	-6.4024E-03	55	2.9750E-02	85	1.3576E-02	115	2.3322E-02
26	3.8329E-02	56	3.5273E-02	86	6.7172E-03	116	1.8608E-02

27	4.3081E-02	57	2.3124E-02	87	2.3029E-02	117	2.2534E-02
28	4.7834E-02	58	2.8698E-02	88	1.6267E-02	118	1.7931E-02
29	1.8091E-02	59	1.7194E-02	89	9.6798E-03	119	1.3416E-02
30	2.3955E-02	60	6.1314E-03	90	1.4373E-02	120	1.7322E-02
31	2.9709E-02	61	1.1881E-02	91	7.9959E-03	121	1.2911E-02
32	4.1033E-03	62	1.3693E-03	92	1.7791E-03	122	8.5828E-03
33	4.0888E-02	63	2.2989E-02	93	1.7222E-02	123	1.2466E-02
34	4.6314E-02	64	2.8359E-02	94	2.1719E-02	124	8.2331E-03
35	5.1632E-02	65	3.3611E-02	95	2.6141E-02	125	4.0784E-03
36	2.9067E-02	66	2.3599E-02	96	3.0491E-02	126	4.5114E-15
37	3.4927E-02	67	2.8856E-02	97	2.4460E-02		
38	1.4330E-02	68	1.9296E-02	98	1.8571E-02		

Table 4. $\Delta E(\max)$, $\Delta E(\max+)$, E_{eff} (Analytic), E_{eff} (KMC) with strong adhesion $f = 0.75$.

N	$\Delta E(\max)/\phi$	$\Delta E(\max+)/\phi$	E_{eff}/ϕ (Analytic)	E_{eff}/ϕ (KMC)	N	$\Delta E(\max)/\phi$	$\Delta E(\max+)/\phi$	E_{eff}/ϕ (Analytic)	E_{eff}/ϕ (KMC)
9	1	2	4.39	2.725007	60	3	5	5.44	6.095752
10	0	1	3.39	2.615396	61	3	6	6.44	6.297837
11	1	1	3.39	2.778875	62	4	6	6.44	6.585454
12	1	2	4.39	2.988714	63	2	5	5.44	4.719845
13	2	4	4.44	4.197006	64	2	4	4.44	3.526861
14	1	3	3.44	3.700747	65	1	4	4.44	3.160087
15	1	3	3.44	3.448595	66	2	4	4.44	3.853471
16	1	3	3.44	3.452431	67	2	4	4.44	4.496483
17	1	3	3.44	3.603812	68	3	5	5.44	4.936934
18	2	4	4.44	4.531417	69	3	5	5.44	5.204049
19	1	3	3.44	3.715621	70	3	5	5.44	5.644064
20	1	3	3.44	3.456839	71	3	6	6.44	6.127802
21	1	3	3.44	3.489495	72	3	5	5.44	5.864287
22	1	3	3.44	3.763647	73	3	6	6.44	6.193006
23	2	4	4.44	4.54257	74	4	6	6.44	6.433234
24	2	4	4.44	4.742128	75	3	6	6.44	6.142301
25	3	5	5.44	5.363361	76	4	6	6.44	6.49023
26	2	4	4.44	3.812829	77	4	7	7.44	6.415716
27	1	4	4.44	3.673562	78	3	5	5.44	4.930902
28	1	3	3.44	3.579002	79	2	5	5.44	3.856305
29	2	4	4.44	4.069252	80	2	4	4.44	3.46775
30	2	4	4.44	4.647959	81	1	4	4.44	3.616927
31	2	4	4.44	5.048493	82	2	4	4.44	4.732014
32	3	5	5.44	5.027681	83	3	5	5.39	5.000544
33	2	4	4.44	4.283069	84	3	5	5.44	5.557813
34	1	4	4.44	3.495385	85	4	5	5.44	5.735602
35	1	3	3.44	3.471428	86	4	7	7.44	6.156445
36	2	4	4.44	4.14488	87	3	5	5.44	5.991286
37	2	4	4.44	4.671747	88	3	6	6.44	6.366895

38	3	5	5.44	5.000252	89	4	6	6.44	6.542923
39	3	5	5.44	4.903743	90	3	6	6.44	6.399141
40	2	5	5.44	4.617529	91	4	6	6.44	6.672519
41	3	6	6.44	4.920517	92	4	7	7.44	6.83212
42	2	4	4.44	3.836599	93	3	5	5.44	4.937629
43	1	3	3.44	3.950523	94	2	5	5.44	4.045375
44	1	3	3.44	3.886212	95	2	4	4.44	3.597248
45	2	4	4.39	4.336656	96	1	4	4.44	3.815837
46	2	4	4.44	4.948072	97	2	4	4.44	4.479961
47	3	5	5.89	5.25538	98	3	6	6.44	5.048184
48	3	5	5.44	5.405564	99	3	5	5.44	5.583762
49	3	6	6.44	5.827405	100	4	6	6.44	5.925287
50	4	6	6.44	6.42211	101	4	7	7.44	6.272987
51	2	5	5.44	4.291569	102	4	6	6.44	6.126492
52	2	4	4.44	3.671632	103	4	7	7.44	6.654272
53	1	4	4.44	3.350325	104	5	7	7.44	6.738924
54	2	4	4.44	3.897465	105	3	6	6.44	5.974716
55	2	4	4.44	4.548468	106	4	6	6.44	6.059756
56	2	4	4.44	5.087336	107	4	7	7.44	6.266179
57	3	5	5.44	5.590862	108	3	6	6.44	6.223578
58	3	5	5.44	5.762445	109	4	7	7.44	6.466588
59	3	6	6.44	5.79078	110	5	7	7.44	6.208408

Table 5. KMC results of diffusion coefficient D_N with weak adhesion $f = 0, 0.05$ at $T = 900K$.

N	$T = 900K$						
	$f = 0$		$f = 0.05$		N	$f = 0$	
	$D_N/(a^2\nu)$		$D_N/(a^2\nu)$			$f = 0.05$	
38	5.7178E-08	1.3630E-07			176	9.8309E-09	1.4364E-08
39	3.1738E-08	9.7780E-08			177	1.1002E-08	1.7117E-08
40	3.6011E-08	1.0505E-07			178	1.1453E-08	1.8522E-08
41	5.3488E-08	1.2405E-07			179	1.2542E-08	1.9596E-08
42	7.9033E-08	1.6603E-07			180	1.6088E-08	2.0916E-08
43	8.1774E-08	1.6731E-07			181	1.5132E-08	2.2151E-08
44	1.0863E-07	2.6763E-07			182	1.8069E-08	2.1396E-08
45	2.0462E-07	3.1351E-07			183	2.0660E-08	2.0456E-08
46	4.2361E-07	5.6415E-07			184	2.0650E-08	1.8117E-08
47	7.9110E-07	7.6538E-07			185	2.0646E-08	1.3569E-08
48	8.6453E-07	9.0244E-07			186	1.9086E-08	8.8031E-09
49	7.4530E-07	7.7198E-07			187	1.7132E-08	6.7018E-09
50	5.1506E-07	5.6946E-07			188	1.3991E-08	5.3717E-09
51	2.6097E-07	4.3904E-07			189	8.9132E-09	3.3449E-09
52	1.4300E-07	2.6265E-07			190	6.1031E-09	2.6789E-09
53	1.3354E-07	2.4758E-07			191	4.6801E-09	2.1891E-09

54	1.5980E-07	2.6693E-07	192	3.0150E-09	2.6669E-09
55	2.8450E-07	3.6099E-07	193	2.6003E-09	3.0304E-09
56	4.7622E-07	4.9507E-07	194	2.3576E-09	2.7213E-09
57	6.7895E-07	5.4312E-07	195	1.3584E-09	2.7365E-09
58	6.3477E-07	4.8155E-07	196	1.3000E-09	2.2220E-09
59	3.6788E-07	3.6288E-07	197	1.0310E-09	2.3777E-09
60	2.2377E-07	2.6347E-07	198	1.0791E-09	2.3263E-09
61	1.3769E-07	2.1831E-07	199	9.4025E-10	2.2444E-09
62	1.4676E-07	2.2500E-07	200	7.8524E-10	1.7612E-09
63	1.8762E-07	2.7660E-07	201	8.2878E-10	1.9360E-09
64	2.9840E-07	4.6077E-07	202	9.2452E-10	1.8156E-09
65	4.9797E-07	5.2262E-07	203	9.4190E-10	1.9719E-09
66	5.6225E-07	4.1803E-07	204	7.8112E-10	1.9925E-09
67	3.8811E-07	2.8322E-07	205	1.0616E-09	1.7122E-09
68	2.0471E-07	1.8573E-07	206	1.3124E-09	1.6407E-09
69	1.4385E-07	1.4324E-07	207	1.2248E-09	1.7096E-09
70	9.9433E-08	9.7492E-08	208	1.2000E-09	2.2410E-09
71	9.5432E-08	8.4206E-08	209	1.9639E-09	2.3184E-09
72	1.0674E-07	9.6865E-08	210	2.1536E-09	2.9622E-09
73	1.2889E-07	1.3371E-07	211	1.2093E-09	2.9486E-09
74	1.0535E-07	1.0712E-07	212	1.1819E-09	3.0871E-09
75	7.1056E-08	9.0118E-08	213	1.8890E-09	3.4795E-09
76	5.4912E-08	7.3807E-08	214	1.8432E-09	3.7088E-09
77	5.0423E-08	8.4075E-08	215	1.9976E-09	4.1010E-09
78	3.0820E-08	7.6405E-08	216	2.5925E-09	4.4338E-09
79	2.1475E-08	7.3302E-08	217	2.2474E-09	4.2609E-09
80	3.1518E-08	7.7452E-08	218	2.7949E-09	5.9202E-09
81	5.0034E-08	9.7841E-08	219	3.2582E-09	5.2504E-09
82	5.5411E-08	9.3073E-08	220	3.5390E-09	6.5212E-09
83	6.7106E-08	1.2166E-07	221	4.4580E-09	7.4257E-09
84	6.8543E-08	1.5063E-07	222	6.1335E-09	8.2579E-09
85	7.2220E-08	1.7031E-07	223	6.4692E-09	1.0361E-08
86	7.2092E-08	1.4682E-07	224	7.9064E-09	9.4780E-09
87	1.1015E-07	1.7727E-07	225	1.0953E-08	1.2768E-08
88	1.2898E-07	1.9237E-07	226	1.2409E-08	1.2567E-08
89	1.6017E-07	1.6358E-07	227	1.1102E-08	1.4182E-08
90	2.0549E-07	1.4509E-07	228	1.3051E-08	9.3747E-09
91	1.5205E-07	1.1421E-07	229	1.2347E-08	8.6715E-09
92	9.1036E-08	8.0574E-08	230	1.3015E-08	7.5562E-09
93	6.8567E-08	6.8186E-08	231	1.1546E-08	5.7722E-09
94	6.0249E-08	6.5004E-08	232	1.1779E-08	3.9400E-09
95	6.6592E-08	9.0901E-08	233	9.0869E-09	4.2766E-09
96	7.0860E-08	1.0641E-07	234	6.4899E-09	3.2102E-09
97	7.1457E-08	1.1469E-07	235	5.6397E-09	3.7360E-09
98	6.4129E-08	1.2090E-07	236	3.9616E-09	3.0974E-09
99	7.6537E-08	1.3977E-07	237	3.8525E-09	3.0959E-09

100	8.7960E-08	1.3511E-07	238	1.9366E-09	3.7582E-09
101	8.9638E-08	1.2550E-07	239	2.0888E-09	3.4831E-09
102	9.0312E-08	9.9107E-08	240	1.8025E-09	3.1639E-09
103	8.9876E-08	8.8026E-08	241	1.7590E-09	3.1915E-09
104	8.9920E-08	5.9648E-08	242	2.1134E-09	4.6171E-09
105	9.0807E-08	6.0004E-08	243	1.9446E-09	4.6546E-09
106	7.0686E-08	5.2858E-08	244	2.2270E-09	4.3585E-09
107	4.4463E-08	5.1344E-08	245	2.8798E-09	4.2396E-09
108	3.6527E-08	4.9903E-08	246	3.0393E-09	4.6208E-09
109	3.8306E-08	6.6299E-08	247	3.7275E-09	5.5926E-09
110	4.3739E-08	7.6074E-08	248	3.9843E-09	5.5270E-09
111	4.9486E-08	6.9969E-08	249	4.3137E-09	5.4469E-09
112	4.8290E-08	9.8686E-08	250	4.8318E-09	5.9862E-09
113	6.0787E-08	8.2016E-08	251	7.9745E-09	6.1007E-09
114	7.5014E-08	7.2147E-08	252	7.3928E-09	6.0849E-09
115	6.3413E-08	6.0833E-08	253	7.6019E-09	4.0924E-09
116	6.2533E-08	4.5605E-08	254	8.4068E-09	3.9709E-09
117	5.4626E-08	2.7505E-08	255	8.5121E-09	4.4251E-09
118	3.9360E-08	2.3317E-08	256	7.0479E-09	3.3818E-09
119	2.8874E-08	1.6352E-08	257	6.2712E-09	3.1772E-09
120	1.9056E-08	1.2568E-08	258	5.6074E-09	2.9132E-09
121	1.1345E-08	1.0623E-08	259	3.9183E-09	2.4741E-09
122	1.0497E-08	1.1215E-08	260	3.3716E-09	2.6576E-09
123	9.3050E-09	1.0814E-08	261	2.6433E-09	2.8956E-09
124	9.3085E-09	1.1969E-08	262	1.9903E-09	2.7020E-09
125	9.7718E-09	1.4266E-08	263	1.7018E-09	2.6504E-09
126	1.1450E-08	1.4647E-08	264	1.6808E-09	3.2928E-09
127	1.3504E-08	1.2405E-08	265	1.7905E-09	3.3323E-09
128	1.4318E-08	1.2821E-08	266	1.6530E-09	3.0993E-09
129	1.9312E-08	1.3219E-08	267	1.8788E-09	3.9048E-09
130	2.3521E-08	1.5049E-08	268	2.0576E-09	3.7798E-09
131	2.4834E-08	1.4422E-08	269	2.3242E-09	3.9575E-09
132	2.7009E-08	1.4219E-08	270	2.7354E-09	4.8349E-09
133	2.1650E-08	1.3204E-08	271	2.8470E-09	4.7179E-09
134	1.8825E-08	1.4459E-08	272	3.3407E-09	4.3398E-09
135	1.5041E-08	1.5471E-08	273	3.8223E-09	4.6663E-09
136	1.5416E-08	2.1059E-08	274	4.9168E-09	5.2209E-09
137	1.4811E-08	1.9620E-08	275	5.3357E-09	5.1703E-09
138	1.7197E-08	2.1240E-08	276	5.9770E-09	4.6346E-09
139	1.8362E-08	2.4252E-08	277	6.6219E-09	4.5292E-09
140	2.0195E-08	2.8685E-08	278	7.5171E-09	3.9568E-09
141	2.1153E-08	3.4128E-08	279	6.4313E-09	3.4930E-09
142	2.3712E-08	3.5389E-08	280	6.6244E-09	2.4242E-09
143	2.4362E-08	4.2180E-08	281	5.7507E-09	2.2499E-09
144	3.1726E-08	4.1938E-08	282	4.7085E-09	1.4894E-09
145	3.4887E-08	4.8489E-08	283	3.4882E-09	1.5417E-09

146	3.9929E-08	4.3935E-08	284	2.5221E-09	1.2376E-09
147	4.4516E-08	4.3945E-08	285	2.1022E-09	1.0074E-09
148	3.9833E-08	3.6322E-08	286	1.6710E-09	8.2471E-10
149	3.5917E-08	2.6912E-08	287	1.3599E-09	1.1026E-09
150	3.2133E-08	2.1718E-08	288	1.1121E-09	1.0624E-09
151	2.7003E-08	1.8002E-08	289	9.6431E-10	6.9640E-10
152	2.0615E-08	1.3957E-08	290	9.5060E-10	7.0445E-10
153	1.5070E-08	1.1895E-08	291	7.7523E-10	9.1963E-10
154	1.1058E-08	1.2111E-08	292	1.0195E-09	8.4515E-10
155	1.1284E-08	1.2922E-08	293	1.0272E-09	6.3828E-10
156	9.6681E-09	1.2917E-08	294	1.0571E-09	6.9076E-10
157	9.9531E-09	1.5658E-08	295	9.5048E-10	1.0085E-09
158	1.1502E-08	1.6762E-08	296	1.1164E-09	8.6795E-10
159	1.3323E-08	1.8982E-08	297	1.0300E-09	7.4559E-10
160	1.4601E-08	2.1952E-08	298	1.0009E-09	6.3612E-10
161	1.8270E-08	2.2560E-08	299	8.8565E-10	1.0193E-09
162	2.0625E-08	2.7331E-08	300	9.5638E-10	7.5796E-10
163	2.3344E-08	2.9992E-08	301	7.7471E-10	4.9254E-10
164	3.0129E-08	3.3689E-08	302	6.3758E-10	5.0622E-10
165	2.8642E-08	3.1423E-08	303	6.9539E-10	4.1456E-10
166	3.1804E-08	2.3513E-08	304	6.1427E-10	5.5125E-10
167	3.6074E-08	2.0673E-08	305	5.1338E-10	7.0195E-10
168	2.4464E-08	1.6366E-08	306	4.4379E-10	6.0823E-10
169	1.9831E-08	1.4318E-08	307	4.5090E-10	7.5653E-10
170	1.3257E-08	1.0966E-08	308	3.7663E-10	7.2281E-10
171	1.1863E-08	1.0690E-08	309	3.5683E-10	8.3731E-10
171	1.1863E-08	1.0375E-08	310	3.3271E-10	8.7858E-10
172	9.6712E-09	1.0660E-08	311	3.2090E-10	1.0946E-09
173	8.9910E-09	1.0962E-08	312	2.3624E-10	1.0206E-09
174	7.9850E-09	1.1987E-08	313	3.4216E-10	1.1835E-09
175	8.2448E-09	1.3482E-08	314	4.5920E-10	1.2742E-09

Table 6. Deviation of energy per atom from continuum value with negligible adhesion $f = 0$.

N	$\delta E/\phi$	N	$\delta E/\phi$	N	$\delta E/\phi$
36	0.056298	129	0.018659	222	0.014554
37	0.040717	130	0.018544	223	0.010759
38	-2.39E-14	131	0.018449	224	0.011467
39	0.012991	132	0.0108	225	0.00773
40	0.02565	133	0.018322	226	0.012882
41	0.037992	134	0.018288	227	0.013588
42	0.050029	135	0.018272	228	0.014293
43	0.038519	136	0.010921	229	0.01063
44	0.050513	137	0.018294	230	0.011352
45	0.039993	138	0.018331	231	0.007744

46	0.051898	139	0.018384	232	0.012793
47	0.042237	140	0.01131	233	0.013512
48	0.054018	141	0.018537	234	0.01423
49	0.065515	142	0.018637	235	0.010691
50	0.05674	143	0.018751	236	0.015662
51	0.048488	144	0.011934	237	0.016377
52	0.021494	145	0.01902	238	0.01709
53	0.033418	146	0.019175	239	0.013618
54	0.026538	147	0.019343	240	0.014346
55	0.03824	148	0.012766	241	0.010923
56	0.031811	149	0.019715	242	0.011666
57	0.043289	150	0.019918	243	0.008291
58	0.054503	151	0.020133	244	0.004949
59	0.048515	152	0.01378	245	0.009802
60	0.042849	153	0.020595	246	0.010555
61	0.021093	154	0.020842	247	0.011307
62	0.032409	155	0.021098	248	0.008024
63	0.027602	156	0.014954	249	0.008788
64	0.038675	157	0.015271	250	0.005551
65	0.034123	158	0.009266	251	0.010311
66	0.044959	159	0.015929	252	0.01107
67	0.04064	160	0.01627	253	0.011827
68	0.021833	161	0.016619	254	0.008645
69	0.032644	162	0.010803	255	0.009413
70	0.028946	163	0.01734	256	0.006274
71	0.025434	164	0.017711	257	0.010945
72	0.035988	165	0.018089	258	0.011708
73	0.032631	166	0.012449	259	0.012468
74	0.029439	167	0.018864	260	0.009381
75	0.013072	168	0.019261	261	0.013984
76	0.02352	169	0.019664	262	0.014739
77	0.020779	170	0.014191	263	0.015493
78	0.018173	171	0.020488	264	0.012456
79	0.003039	172	0.020908	265	0.013219
80	0.013345	173	0.021333	266	0.010222
81	0.035803	174	0.016017	267	0.010995
82	0.021186	175	0.016485	268	0.008035
83	0.031075	176	0.011276	269	0.005101
84	0.028878	177	0.017435	270	0.0096
85	0.026788	178	0.017916	271	0.010378
86	0.01317	179	0.018402	272	0.011155
87	0.022905	180	0.013335	273	0.008266
88	0.021104	181	0.013859	274	0.009052
89	0.030628	182	0.008891	275	0.006199
90	0.028876	183	0.014915	276	0.010616
91	0.038198	184	0.015448	277	0.011395

92	0.036492	185	0.015984	278	0.012172
93	0.034866	186	0.011147	279	0.009362
94	0.02268	187	0.022412	280	0.010146
95	0.031843	188	0.017609	281	0.00737
96	0.03044	189	0.018155	282	0.015255
97	0.029105	190	0.013441	283	0.012487
98	0.017631	191	0.01402	284	0.013263
99	0.026629	192	0.009392	285	0.010527
100	0.025484	193	0.015183	286	0.01131
101	0.024397	194	0.015767	287	0.008607
102	0.013563	195	0.016353	288	0.005926
103	0.022391	196	0.011839	289	0.010186
104	0.021467	197	0.012454	290	0.010972
105	0.030117	198	0.00802	291	0.011756
106	0.029203	199	0.008662	292	0.009112
107	0.028336	200	0.004306	293	0.009902
108	0.018257	201	-7.92E-15	294	0.007289
109	0.026742	202	0.005645	295	0.008086
110	0.026011	203	0.006315	296	0.005502
111	0.025321	204	0.006985	297	0.009673
112	0.015744	205	0.002778	298	0.010463
113	0.024063	206	0.008327	299	0.01125
114	0.02349	207	0.008998	300	0.008701
115	0.022955	208	0.009669	301	0.009495
116	0.013834	209	0.005556	302	0.006974
117	0.021988	210	0.011012	303	0.007774
118	0.021554	211	0.011683	304	0.005281
119	0.021152	212	0.012354	305	0.002807
120	0.012447	213	0.008331	306	0.006888
121	0.020438	214	0.013697	307	0.007688
122	0.020125	215	0.014368	308	0.008486
123	0.01984	216	0.015039	309	0.006044
124	0.011516	217	0.011101	310	0.006847
125	0.019348	218	0.011793	311	0.004432
126	0.01914	219	0.007918	312	0.00524
127	0.018957	220	0.013175	313	0.00285
128	0.010984	221	0.013865	314	0.000478

Table 7. $\Delta E(\max)$ for negligible adhesion $f = 0$.

N	$\Delta E(\max)/\phi$	N	$\Delta E(\max)/\phi$	N	$\Delta E(\max)/\phi$
38	5	88	3	182	6
39	5	90	4	186	5
40	5	94	4	192	6
41	5	98	4	201	8
43	4	102	4	205	7

45	4	104	4	209	7
47	3	108	5	213	6
48	3	112	5	219	7
52	5	116	4	225	7
54	4	120	6	231	5
56	3	124	6	235	6
57	2	128	6	244	8
61	5	132	6	250	7
63	4	136	6	256	5
65	3	140	5	260	6
68	4	144	6	269	7
70	4	148	6	275	7
71	4	152	6	281	5
75	5	158	5	288	7
79	6	162	5	294	7
80	5	166	5	296	7
82	4	170	6	305	9
86	4	176	5	314	10

Table 8. KMC results of diffusion coefficient D_N with strong adhesion $f = 0.50$ at $T = 700K$ and $900K$.

N	$f = 0.50$				
	$D_N/(a^2\nu)$		N	$D_N/(a^2\nu)$	
	700K	900K		700K	900K
9	2.7678E-06	3.1898E-05	45	1.0081E-10	3.4107E-08
10	1.0568E-06	1.5890E-05	46	9.4660E-11	3.0658E-08
11	2.1912E-07	5.8022E-06	47	6.6890E-11	3.1366E-08
12	3.5808E-08	2.2606E-06	48	7.1077E-11	3.3961E-08
13	1.8286E-08	1.4183E-06	49	1.1526E-10	3.8385E-08
14	1.0972E-07	3.6071E-06	50	2.3332E-10	4.8154E-08
15	8.3412E-07	8.8583E-06	51	2.6534E-10	5.6996E-08
16	1.8072E-07	4.3265E-06	52	3.6697E-10	8.7150E-08
17	4.6822E-08	2.0607E-06	53	6.1724E-10	1.6134E-07
18	1.6906E-08	1.0774E-06	54	2.5698E-09	3.1768E-07
19	3.4517E-08	1.4614E-06	55	2.0972E-08	5.7561E-07
20	6.5152E-08	2.6140E-06	56	1.7957E-08	3.2383E-07
21	4.1185E-07	5.0131E-06	57	2.7511E-09	1.1372E-07
22	7.9352E-08	2.2707E-06	58	3.1475E-10	4.3721E-08
23	3.7693E-08	1.1559E-06	59	8.2231E-11	2.5449E-08
24	7.5326E-09	5.9464E-07	60	7.1347E-11	2.0987E-08
25	4.1706E-09	3.5416E-07	61	3.8905E-11	1.8474E-08
26	1.7429E-09	2.2358E-07	62	6.8436E-11	1.7175E-08
27	7.1490E-10	1.2663E-07	63	5.6361E-11	1.9203E-08
28	6.1871E-10	1.1742E-07	64	4.9900E-11	2.2138E-08
29	1.6480E-09	2.9655E-07	65	4.7516E-11	2.3483E-08

30	3.0229E-08	1.2104E-06	66	5.8553E-11	3.6674E-08
31	2.0211E-07	2.2619E-06	67	1.9196E-10	7.9708E-08
32	6.4626E-08	1.0857E-06	68	9.9410E-10	2.0488E-07
33	7.0627E-09	4.0838E-07	69	1.1668E-08	3.8879E-07
34	1.2348E-09	1.5626E-07	70	2.5923E-08	2.8263E-07
35	4.0527E-10	1.0147E-07	71	6.7407E-09	1.1528E-07
36	2.4047E-10	6.7142E-08	72	3.8508E-10	3.5349E-08
37	3.4051E-10	9.9013E-08	73	4.8509E-11	1.1526E-08
38	6.1153E-10	1.8864E-07	74	1.3822E-11	6.1621E-09
39	1.0922E-08	7.0162E-07	75	7.5618E-12	4.6881E-09
40	5.4002E-08	1.4006E-06	76	7.7250E-12	4.1802E-09
41	7.6181E-08	9.8744E-07	77	4.3375E-12	3.2571E-09
42	6.5177E-09	3.2555E-07	78		4.1203E-09
43	9.4118E-10	1.0220E-07	79		3.9682E-09
44	2.2152E-10	4.6757E-08	80		3.8531E-09

Table 9. KMC results of diffusion coefficient D_N with moderate adhesion $f = 0.17$ mimicking Ag/MgO(001) at $T = 900K$.

$T = 900K; f = 0.17$					
N	$D_N/(a^2\nu)$	N	$D_N/(a^2\nu)$	N	$D_N/(a^2\nu)$
38	3.7518E-07	63	3.6137E-07	88	1.6361E-07
39	4.8375E-07	64	3.4843E-07	89	1.8233E-07
40	7.1508E-07	65	3.6873E-07	90	1.8675E-07
41	1.1791E-06	66	3.3496E-07	91	2.2312E-07
42	1.4810E-06	67	4.0763E-07	92	2.2478E-07
43	1.9547E-06	68	4.8080E-07	93	1.8839E-07
44	1.4683E-06	69	4.9993E-07	94	1.5631E-07
45	1.2057E-06	70	5.0174E-07	95	1.8162E-07
46	6.8049E-07	71	3.3141E-07	96	1.3909E-07
47	5.9876E-07	72	2.8024E-07	97	1.4831E-07
48	4.7542E-07	73	2.4749E-07	98	1.5224E-07
49	4.8813E-07	74	2.1654E-07	99	1.1646E-07
50	6.0239E-07	75	1.9162E-07	100	1.3535E-07
51	7.7779E-07	76	2.2819E-07	101	1.3971E-07
52	8.5744E-07	77	2.3806E-07	102	1.4198E-07
53	7.5689E-07	78	1.9449E-07	103	1.2814E-07
54	6.0444E-07	79	1.6624E-07	104	1.2917E-07
55	4.8134E-07	80	1.3545E-07	105	1.1632E-07
56	3.6766E-07	81	1.2821E-07	106	8.9139E-08
57	3.8403E-07	82	1.4314E-07	107	8.4382E-08
58	5.0759E-07	83	1.6218E-07	108	6.8694E-08
59	6.2175E-07	84	1.6739E-07	109	5.3883E-08
60	4.7906E-07	85	1.6408E-07	110	4.0658E-08
61	4.6467E-07	86	1.7889E-07		
62	3.5165E-07	87	1.6551E-07		

Table 9. KMC results of diffusion coefficient D_N with larger sizes N moderate adhesion $f = 0.75$ at $T = 900K$.

N	$D_N/(a^2v)$	N	$D_N/(a^2v)$
174	4.986E-08	400	1.916E-09
190	1.208E-08	451	4.156E-09
200	3.256E-08	502	4.853E-09
220	1.194E-08	559	2.431E-09
255	2.147E-08	595	2.253E-10
290	2.070E-08	616	1.456E-09
330	1.344E-08	658	3.699E-10
355	1.447E-09	728	7.569E-10
370	7.905E-09	798	6.236E-10